Biochimica et Biophysica Acta 1832 (2013) 1294–1303

Contents lists available at SciVerse ScienceDirect

Biochimica et Biophysica Acta

journal homepage: www.elsevier.com/locate/bbadis

miR-135a targets IRS2 and regulates insulin signaling and glucose uptake in the diabetic gastrocnemius skeletal muscle

Priyanka Agarwal [a,c], Rohit Srivastava [b], Arvind K. Srivastava [b], Shakir Ali [c], Malabika Datta [a,*]

[a] CSIR-Institute of Genomics and Integrative Biology, Mall Road, Delhi-110 007, India
[b] CSIR-Central Drug Research Institute, Chattar Manzil, Lucknow-226 001, India
[c] Department of Biochemistry, Jamia Hamdard, Hamdard Nagar, New Delhi-110 062, India

ARTICLE INFO

Article history:
Received 18 January 2013
Received in revised form 6 March 2013
Accepted 13 March 2013
Available online 8 April 2013

Keywords:
miR-135a
Diabetes
IRS2
Insulin
Microarray
Skeletal muscle

ABSTRACT

Although aberrant miRNA signatures are associated with diabetes, yet, the status and role of altered miRNAs in the diabetic skeletal muscle is currently poorly understood. Here, we report that 41 miRNAs are altered in the diabetic gastrocnemius skeletal muscle and of these, miR-135a that is identified as a critical regulator of myogenesis, is significantly up-regulated. IRS2 is predicted as its potential putative target and its levels are down-regulated in the diabetic gastrocnemius skeletal muscle. In C2C12 cells, while miR-135a levels decreased during differentiation, IRS2 levels were up-regulated. miR-135a significantly reduced IRS2 protein levels and its 3′UTR luciferase reporter activity and these were blunted by the miR-135a inhibitor and mutation in the miR-135a binding site. Knock-down of endogenous miR-135a levels increased IRS2 at the mRNA and protein levels. miR-135a also attenuated insulin stimulated phosphorylation and activation of PI3Kp85α and Akt and glucose uptake. miR-135a levels were also found to be elevated in the human diabetic skeletal muscle. *In-vivo* silencing of miR-135a alleviated hyperglycemia, improved glucose tolerance and significantly restored the levels of IRS2 and p-Akt in the gastrocnemius skeletal muscle of db/db mice without any effect on their hepatic levels. These suggest that miR-135a targets IRS2 levels by binding to its 3′UTR and this interaction regulates skeletal muscle insulin signaling.

1. Introduction

MicroRNAs (miRNAs) are a class of small (~22 nucleotides) non-coding RNA species that act by regulating the expression of their target genes by either mRNA degradation or translational repression [1]. Since their discovery in *Caenorhabditis elegans* [2], miRNAs are now believed to participate in diverse physiological cellular pathways. In addition to being involved in cellular phenomena like differentiation, proliferation and cell signaling [3], miRNAs are also being increasingly implicated in several pathological states [4].

Type 2 diabetes (T2D) is a complex multi-factorial disease that sets in due to decreased responsiveness of the peripheral target tissues to insulin (insulin resistance). The resulting hyperglycemia triggers the pancreatic β-cells that initially try to rescue this state by increasing insulin synthesis and secretion. But when the insulin resistant condition and hyperglycemia persist, these lead to pancreatic β-cell toxicity and cell death. Of the insulin target tissues, skeletal muscle insulin resistance is believed to be an early event during the onset and progression to diabetes [5]. Almost 80% of insulin stimulated glucose disposal occurs in the skeletal muscle [6,7] and therefore, this tissue getting insulin resistant contributes to the pathogenesis of the overall insulin resistant state. Skeletal muscle glucose uptake is regulated by the metabolic pathways of glycolysis (~90% of which corresponds to glucose oxidation) and glycogen synthesis [8].

Skeletal muscle insulin resistance that primarily involves the glycogen synthetic machinery [9,10] is the earliest visible metabolic defect during the onset of the disease [11,12]. Additionally, skeletal muscle insulin resistance also promotes atherogenic dyslipidemia and contributes to the development of other deregulations associated with the metabolic syndrome [13]. Therefore, by virtue of it being the most important tissue involved in whole body glucose homeostasis [14], it is imperative that the mechanisms involved in skeletal muscle insulin resistance are studied in detail.

Diverse mechanisms have been identified as underlying factors responsible for skeletal muscle insulin resistance. The emergence of miRNAs as critical metabolic regulators has added another mechanistic layer of regulation and suggests a possible role of these RNA species in this defect of the skeletal muscle. Several reports describe altered miRNome signatures during diabetes [15–19] and these, together with other studies that describe the contribution of very specific miRNAs in diverse metabolic processes linked to T2D [4], suggest that miRNAs play crucial roles during the onset and progression of this complex metabolic disease. However, despite the skeletal muscle being a critical contributing tissue in diabetes, very few studies

* Corresponding author. Tel.: +91 11 27667439, +91 11 27667602x135; fax: +91 11 27667471.
E-mail address: mdatta@igib.res.in (M. Datta).

0925-4439/$ – see front matter © 2013 Elsevier B.V. All rights reserved.
http://dx.doi.org/10.1016/j.bbadis.2013.03.021

describe the role and status of miRNAs in the diabetic skeletal muscle [15–17]. In a recent study, miRNA profiling in the skeletal muscle of control and diabetic subjects was studied and 29 miRNAs were up-regulated and 33 were down-regulated [15]. Of these, miRNAs that depict skeletal muscle specific expression were preferentially down-regulated suggesting that an altered miRNA signature might have relevance in the diabetic skeletal muscle. In a diabetic GK rat model, 7 miRNAs were down-regulated and 2 were up-regulated in the skeletal muscle [16]. miR-24 was one of the up-regulated miRNAs and its target, p38MAPK was markedly down-regulated suggesting that these events might contribute to the altered physiology of the diabetic skeletal muscle. Apart from these few reports, the significance and role of miRNAs in the skeletal muscle during diabetes has not been studied enough. Therefore, there is a need for detailed analysis of miRNAs in the diabetic skeletal muscle so that a comprehensive role of these small RNA species in this tissue during diabetes could be unraveled.

In the present study, we report an altered miRNA signature in the gastrocnemius skeletal muscle of db/db mice. These mice are believed to exhibit a pattern of diabetes progression that is strikingly similar to that in humans [20]. Our data show that 41 miRNAs are differentially regulated; of which 10 and 31 miRNAs were significantly up- and down-regulated, respectively. One of the key altered miRNAs was miR-135a. miR-135a has been shown to be critical in myogenesis by targeting the specific transcription factor, myocyte enhancer factor 2C (MEF2C) [21] and its levels are up-regulated in the degenerative phase of muscle damage [22]. In this study, we sought to evaluate the consequence of elevated miR-135a levels in the diabetic gastrocnemius skeletal muscle. Our results show that miR-135a targets IRS2 and consequently abrogates insulin signaling and glucose uptake in skeletal muscle cells that is a critical factor towards initiation of the diabetic phenotype. This was substantiated by the observation of significant alleviation of hyperglycemia and improvement of glucose tolerance by *in-vivo* silencing of miR-135a in db/db mice.

2. Materials and methods

2.1. Animals

Twelve week old male normal (C57BL/KsJ-lepr^{db}/$^{+}$) and diabetic (C57BL/KsJ lepr^{db}/lepr^{db}) mice were obtained from the Animal House Facility of the CSIR-Central Drug Research Institute, Lucknow, India. The handling and maintenance of these animals (n = 4 from each group) have been described in a recent report from our laboratory [18]. The gastrocnemius skeletal muscles were dissected and collected in RNA later and stored at −80 °C until further use in all subsequent experiments that were carried out at the CSIR-Institute of Genomics and Integrative Biology, Delhi, India. All procedures were carried out in accordance with the guidelines of the Institutional Animal Ethical Committee and all experiments were approved by the same.

2.2. RNA extraction and miRNA microarray

Total RNA from the gastrocnemius skeletal muscle (n = 4) was extracted using Trizol (Invitrogen, Carlsbad, CA, USA) following the manufacturer's protocol and quantified with a NanoDrop spectrophotometer (ND-1000, NanoDrop Technologies, DE, USA). Ratios of OD 260/280 were between 1.9 and 2.0. The integrity of RNA samples was determined in a Bioanalyzer 2100 (Agilent, CA, USA) and all samples had RIN values in the range of 8.0–8.5.

Microarray experiments for four animals in each group were carried out with the mouse miRNA 8 × 15K array from Agilent by Genotypic Technology Pvt. Ltd. Bangalore, India. Total RNA (100 ng) was de-phosphorylated and the subsequent denaturation, ligation and hybridization steps were performed according to the manufacturer's instructions. Slides were scanned on a microarray scanner (G2565BA, Agilent) at 100 and 5% XDR settings. Agilent Feature Extraction software (v9.3.5) was used to extract the raw data. All experiments were according to the MIAME guidelines and the data that were analyzed by the method as described below have been deposited to the GEO database. The GEO accession number for the same is GSE32376.

2.3. Target prediction and pathway analysis

Predicted targets of miR-135a as extracted from miRanda (http://www.microRNA.org/), Target Scan (http://www.targetscan.org/) and PicTar (http://www.PicTar.org/) were used to identify the potential putative targets of this miRNA. The common targets predicted by all the three tools were analyzed for the cellular pathways that they enrich in using DAVID and KEGG mapping databases that categorize a set of genes from an input genes' list on the basis of annotation similarity and then map them as significantly over-represented in a biological pathway. These suggest that the enriched pathway might play a role in the physiological condition being considered.

2.4. Cloning and mutagenesis

The IRS2 3′UTR was amplified using sequence specific primers flanking the miR-135a binding site (sense: 5′ CCGCTCGAGGTACCC TGGGAGGAGGTGAT 3′ and antisense: 5′ ATAAGAATGCGGCCGCTT TCAACATGGCGGCGATG3′). The PCR product was cloned downstream of the renilla luciferase gene within the psiCHECK™-2 reporter vector (Promega, MA, USA) according to the manufacturer's protocol. This vector harbors an intraplasmid firefly luciferase cassette that is used as the normalization reporter control. Mutation in the miR-135a binding site (GCCA → TCTA) in the IRS2 3′UTR was generated with mutation primers (sense:5′ CCAGCCCCATCGCCTCTATGTTGAAAGCG GC 3′ and antisense: 5′ GCCGCTTTCAACATAGAGGCGATGGGGCTGG 3′) (under-lined regions depict the mutated sites) using the Quickchange XL site-directed mutagenesis kit (Stratagene, CA, USA). Presence of the inserts and incorporation of the mutation were confirmed by sequencing.

2.5. Cell culture

The C2C12 mouse myoblast cell line was obtained from the National Center for Cell Science (NCCS), Pune, India. Cells were maintained in Dulbecco's modified Eagle's medium (DMEM) supplemented with 10%fetal bovine serum and 10 units/ml penicillin/streptomycin/glutamine. At a confluence of 70–80%, the medium was replaced with DMEM supplemented with 0.5% fetal bovine serum (differentiation medium) and 10units/ml penicillin/streptomycin/glutamine to promote myoblast differentiation into myotubes that were evident after four days of incubation.

2.6. Quantitative real-time PCR (qRT-PCR) analyses

miR-135a levels were assessed in mice gastrocnemius skeletal tissues (normal and diabetic) and C2C12 cells (undifferentiated and differentiated) using SYBR Green (Applied Biosystems, CA, USA) and miRNA specific primers (Forward Primer: 5′ACACTCCAGCTGGGTATG GCTTTTTATTCCT3′ and universal Reverse primer: 5′GGTGTCGTGGA GTCGGCAA3′). RNA (2 μg) from the skeletal tissues was reverse transcribed using the specific miR-135a stem-loop RT primer (5′ CTCAACTGGTGTCGTGGAGTCGGCAATTCAGTTGAGTCACATAG3′) and then subjected to quantitative PCR with SYBR Green. The specificity of the amplified products was assessed by the dissociation curve analysis in an ABI PRISM 7500 thermal cycler. Data was analyzed using the Pfaffl method [23] and normalized to U6 snRNA. Reactions from each animal (n = 4) of both groups were run in triplicate. For quantitation of miR-135a levels in C2C12 cells, total RNA (2 μg) from

undifferentiated and differentiated C2C12 cells were reverse transcribed and subjected to RT-PCR as described above. All experiments were done in triplicate and normalized to U6 snRNA.

2.7. Transfection of miR-135a

Differentiated C2C12 cells were transfected with the scramble or miR-135a mimic (25–100 nM) and miR-135a inhibitor (50 nM) (Dharmacon, Lafayette Colorado, USA) using Lipofectamine 2000 (Invitrogen, CA, USA). The inhibitor used is a non-hydrolysable single-stranded reverse complement of miR-135a with flanking hairpin structures and it acts by irreversible binding to the mature form of miR-135a and thereby preventing its binding to the target. After 48 h, cells were harvested and subjected to RT-PCR and Western Blot analyses as described below.

2.8. Quantitative real time-PCR (qRT-PCR) for IRS2 and Western Blot analyses

The levels of IRS2 at the protein level were assessed by Western Blot in cells transfected with the miR-135a mimic and its inhibitor. 50 μg protein of each incubation was resolved on SDS-PAGE, transferred to nitrocellulose membranes and IRS2 levels were detected with anti-IRS2 antibody. Endogenous miR-135a levels were knocked down by transfecting miR-135a inhibitors (50 and 100 nM) and on termination of incubation (48 h), the levels of IRS2 (at the mRNA and protein level) were determined. For IRS2 mRNA levels, 2 μg of total RNA was reverse transcribed and the levels of IRS2 mRNA were determined by quantitative RT-PCR using gene-specific primers (sense: 5′ CTGCGTCCTCTCCCAAAGTG 3′ and antisense: 5′ GGGGT CATGGGCATGTAGC 3′). 18S rRNA and β-actin were taken as the loading controls for qRT-PCR and Western Blot analyses, respectively. To study the effect of miR-135a on insulin signaling, cells were transfected with miR-135a (100 nM) and/or its inhibitor and after 48 h, cells were incubated with or without insulin (100 nM) for 20 min, pelleted down, lysed in cell lysis buffer (Sigma, St. Louis, USA) and lysates were centrifuged at 15,000 *g* for 15 min. 50 μg protein (supernatant) of each incubation was resolved on SDS-PAGE, transferred to nitrocellulose membranes and probed with Akt, p-Akt, PI3Kp85α (Santa Cruz, CA, USA) and p-PI3Kp85α (Cell Signaling, MA, USA) antibodies. Immuno-reactive bands were detected by BCIP-NBT. β-actin (Santa Cruz) was taken as the loading control. The mRNA and protein levels of IRS2 in normal and diabetic (db/db) mice gastrocnemius skeletal muscle was also detected in an identical manner.

2.9. Luciferase activity assay

For the luciferase assay to validate IRS2 as a target of miR-135a, HEK cells (approximately 75,000 cells) were seeded in 12-well plates and used for the experiment. HEK cells were chosen because they express low levels of miR-135a [24]. Cells were transfected with either the scramble or various doses of the miR-135a mimic (5–50 nM). 150 ng of the wild type (psiCHECK2-IRS2-UTR) or mutant (psiCHECK2-IRS2-UTR-mut) IRS2 3′UTR or the vector alone were co-transfected using Lipofectamine 2000 according to the manufacturer's instructions. After 48 h, cells were lysed and firefly and *Renilla* luciferase activities were measured using the dual-luciferase reporter assay kit (Promega, MA, USA) on a luminometer (Orion II, Luminometer, Germany). To check the specificity of the miR-135a effect, HEK cells were co-transfected with psiCHECK2-IRS2-3′ UTR (150 ng wild type or mutant) and miR-135a mimic (25 nM) and its inhibitor (10 nM) and the luciferase activities were measured. Control cells were transfected with the scramble sequence. Renilla reporter luciferase activity was normalized to firefly luciferase activity.

2.10. 2-(N-(7-nitrobenz-2-oxa-1,3-diazol-4-yl)amino)-2-deoxy-D-glucose (2-NBDG) uptake assay

The effect of miR-135a and its inhibitor on insulin stimulated glucose uptake was assessed by 2-NBDG uptake. Differentiated C2C12 cells were transfected with miR-135a and its inhibitor as described above. After 48 h, cells were pre-incubated in 0.05% glucose containing Krebs Ringer Bicarbonate buffer (pH 7.4 with 2%BSA). After this pre-incubation at 37 °C for 30 min, cells were incubated in the presence or absence of insulin (100 nM) for 10 min and then further treated with insulin and 500 μM of 2-NBDG (Invitrogen, CA, USA) for 2 h at 37 °C in glucose-free Krebs Ringer Bicarbonate buffer containing 2% BSA. On termination of incubation, the cells were washed with cold phosphate-buffered saline (PBS) and 2-NBDG uptake into the cells was assayed by FACS analysis (BD Biosciences, USA). Results are expressed as Fluorescence Intensity (arbitrary units) of the various treatments with respect to the control.

2.11. Microarray data analysis

Raw data was extracted using the Agilent Feature Extraction software (V9.3.5) and was normalized using quantile normalization in the R language (version 2.14.0, http://www.r-project.org/). Values were then log2 transformed and median centered across miRNAs and samples. Z-score statistical test was applied to the normalized data and miRNAs having a Z-score less than or equal to −1.96 (that is inferred as a significance of $p < 0.05$) were considered as down-regulated and those greater than or equal to +1.96, as up-regulated miRNAs.

2.12. miR-135a levels in the normal and diabetic human skeletal muscle

Total RNA from age (65–75 years) and sex matched (male) normal and type 2 diabetic human skeletal muscle (n = 3 each) were purchased from M/S. Biochain Life Sciences (Newark, CA, USA). All tissues were collected by M/S. Biochain with informed consent from the donors and their relatives and according to the approval of M/S. Biochain's Regulatory Board. The glucose levels of the normal individuals were 4.7 ± 2.02 mM and those of the diabetic individuals were 12.59 ± 1.15 mM. Total RNA (2 μg) of each individual was reverse transcribed and quantified for miR-135a levels using Real-Time PCR as described above in a StepOne Plus RT-PCR system (Applied Biosystems, CA, USA). U6 snRNA was used for normalization. RNA from each individual was run in triplicate and data were analyzed as described above.

2.13. In-vivo studies with miR-135a antagomir

To validate if miR-135a inhibition could normalize the diabetic status *in vivo*, experiments were done in the normal and diabetic db/db mice. Animals (n = 5 in each group) were divided into three groups: normal db/+ mice injected with scramble; diabetic db/db mice injected with scramble and db/db mice injected with antagomir-135a. Chemically modified HPLC purified miR-135a antagomirs (5′ C*A*CAUAGGA AUAAAAA GCC*A*U*A*-chol3′ where all bases were 2-O′methyl modified phosphoramidites, "*" represents phosphorothioate linkages, and "-Chol" refers to cholesterol moiety) and scramble (5′ G*A*CUC CACUCUUCUAGAAU*A*A*C*-chol3′) with the same modifications were synthesized and purchased from Dharmacon (Lafayette, CO, USA). All oligos (antagomir or scramble) were dissolved in saline and injected through the tail vein (100 μl) for three consecutive days at a dose of 80 mg/kg body weight [25]. Random blood glucose levels of fed animals were measured at the start of the experiment (day 0) and on each day of the three consecutive days of the experiment (ACCU-CHEK, Roche). After 24 h of the last injection i.e. on the fourth day, oral glucose tolerance test (OGTT) was performed after an overnight fasting period. All animals were given an oral dose of glucose at a dose of 3 g/kg body weight and the blood glucose levels were

measured at 0, 30, 60, 90 and 120 min. Animals were euthanized the next day and the gastrocnemius skeletal muscle and liver tissues were dissected and the levels of IRS2, p-Akt and Akt were determined by Western Blot as described above.

2.14. Densitometry analysis

Protein expression was evaluated by densitometric analysis performed with Alpha DigiDoc 1201 software (Alpha Innotech Corporation, CA, USA). The same size rectangle box was drawn surrounding each band and the intensity of each was analyzed by the program after subtraction of the background intensity.

2.15. Statistical analysis

All experiments were done thrice and data are expressed as means ± SEM. Values represent the means of at least three independent experiments. The statistical significance of differences was evaluated with the Student's t-test and p-values of at least <0.05 are considered statistically significant.

3. Results

3.1. miR-135a levels are up-regulated in the gastrocnemius skeletal muscle of db/db mice

To evaluate miRNA expression signatures in the gastrocnemius skeletal muscle of db/db mice, we performed a miRNA microarray using the miRNA mouse array from Agilent Technologies (CA, USA). Gastrocnemius skeletal muscle tissues of four animals each from the normal (db/+) and diabetic (db/db) group were taken. As shown in Fig. 1A, a total of 41 miRNAs were altered in the diabetic skeletal muscle as compared to that of the normal mice. Of these, 10 miRNAs were up-regulated and 31 miRNAs were down-regulated with a p-value <0.05. Predicted targets of all these altered miRNAs were extracted from TargetScan, miRanda and PicTar and miRNAs that had targets predicted by one or more algorithms are shown in Fig. 1B. Only miR-135a and miR-18a had targets predicted by all the three algorithms. This, however, does not exclude the possibility that the other miRNAs that did not occupy the common intersection area, could be of relevance to diabetes. Since prediction algorithms use specific criteria for target prediction and might be prone to generation of false positives, we followed a common procedure of prioritizing on the miRNAs that occupy the intersection area to increase the confidence of subsequent validation and functional relevance [26,27].

We then did a pathway analysis of these common predicted targets (of miR-135a and miR-18a) using the DAVID and KEGG pathway mapping databases. These tools assign significant over-representation of pathways using annotation based enrichment of genes from an input list *versus* those that are represented in the whole genome. While miR-135a targets mapped onto different pathways, those of miR-18a did not converge onto any common significant over-represented pathway. Importantly, among the pathways overrepresented by the targets of miR-135a, the type 2 diabetes pathway (corrected p value = 1.20E−04) was the topmost significant pathway (Fig. 1C). miR-135a, therefore, was prioritized for evaluation of a possible role in diabetes.

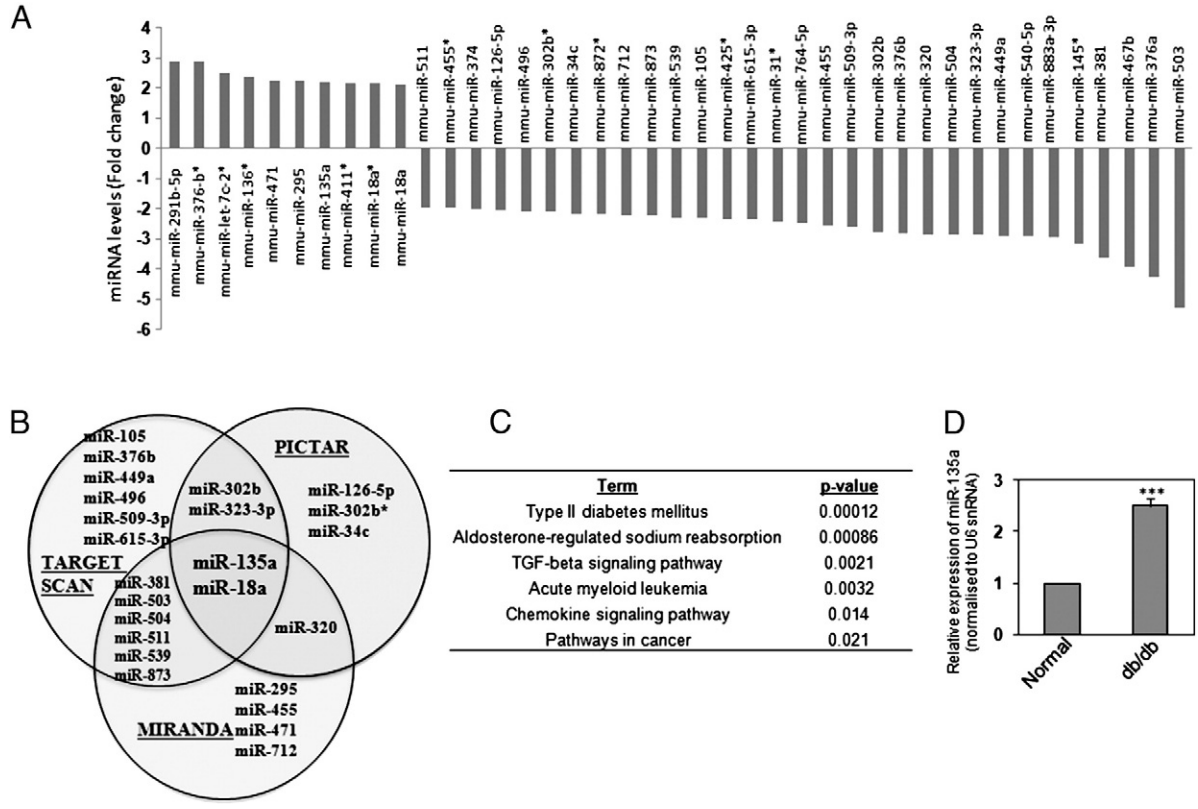

Fig. 1. Levels of miR-135a in normal and diabetic mice skeletal muscle and the pathways that its targets enrich in. (A) Differentially altered miRNAs in the diabetic mice skeletal muscle that were identified by miRNA microarray. The fold change of the individual miRNAs with respect to their levels in the normal mice is represented. Microarray hybridization was done with tissues from four animals each of the normal and diabetic group. (B) Targets to the altered miRNAs as in "A" were extracted from TargetScan, PicTar and miRanda and the miRNAs that are predicted to have targets in one or more algorithms are shown. (C) Common targets of miR-135a from TargetScan, PicTar and miRanda were classified into the pathways they enrich in using DAVID and KEGG mapping databases and the significant ($p < 0.05$) pathways with their values of significance are listed. (D) Relative expression of miR-135a in the skeletal muscle of normal (db/+) and diabetic (db/db) mice as evaluated by quantitative Real Time-PCR. Total RNA (2 μg) from each of the normal and diabetic tissue were reverse transcribed and subjected to quantitative Real-Time PCR as described in the 'Materials and methods' section. Values in 'D' are means ± SEM of triplicate experiments from each animal. ***$p < 0.001$ as compared to normal (non-diabetic) mice.

Also, it was one of the significantly up-regulated miRNAs in the db/db gastrocnemius skeletal muscle and is identified as a critical regulator of myogenesis by targeting MEF2C, a transcription factor that actively regulates several muscle specific genes [21,28]. We, therefore, further sought to assess the functional relevance of the elevated levels of miR-135a in the diabetic gastrocnemius skeletal muscle. The up-regulated status of miR-135a was validated by quantitative real time PCR and as in the microarray, miR-135a levels depicted a significant increase in the muscle of db/db mice as compared to normal mice (Fig. 1D).

As stated above, the pathway term: type 2 diabetes mellitus was the topmost significant pathway overrepresented by the set of common targets of miR-135a. Although the "type 2 diabetes" pathway refers to diverse converging metabolic pathways, the targets of miR-135a were majorly enriched amongst the significant contributory pathways of insulin signaling, adipocytokine signaling and pancreatic insulin synthesis and secretion (Fig. 2A). Within these, most of the targets centered on the insulin signaling pathway wherein defects at one or more points are believed to be strongly associated with insulin resistance and diabetes. IRS2 was one such miR-135a predicted target that belonged to this pathway. IRS2 occupies a major upstream position in the insulin signaling pathway, acts as a docking intermediate between the insulin receptor and other SH2 (src homology) domain containing intracellular molecules and its disruption causes type 2 diabetes [29,30]. These imply that inhibited levels of IRS2 are a major determinant of the diabetic status of an individual and being a predicted target of miR-135a, the elevated levels of miR-135a might lead to decreased IRS2 levels. We, therefore, sought to evaluate whether IRS2 is a validated target of miR-135a and if so, the physiological relevance of this interaction. The region from 2285 to 2290 nucleotides on the 3′UTR of IRS2 harbors the binding site for miR-135a (Fig. 2B) and this corresponds to nucleotide positions of 23–28 on the mouse IRS2 3′UTR. We therefore, subsequently assessed the status of IRS2 in the normal and diabetic mice gastrocnemius skeletal muscle. As shown in Fig. 2C and D, the levels of IRS2 were significantly down-regulated both at the transcript and protein level in the gastrocnemius skeletal muscle of the db/db mice as compared to those of normal mice, a pattern inverse to that of miR-135a (Fig. 1D). These indicated that the elevated levels of miR-135a might be responsible for the decreased levels of IRS2 in the db/db mice gastrocnemius skeletal muscle.

3.2. miR-135a levels are inhibited in differentiated C2C12 cells and they regulate IRS2 levels by binding to its 3′UTR

To further validate the miR-135a–IRS2 interaction and to evaluate the consequences of this miRNA-target pair, we used C2C12 cells that were differentiated using 0.5% serum containing growth media. During this process of differentiation, undifferentiated myoblast cells that are mononuclear and fusiform-shaped acquire a multinuclear and tubular phenotype and become more insulin sensitive [31]. To validate whether miR-135a targets IRS2, we initiated by evaluating the levels of miR-135a and its predicted target, IRS2 in undifferentiated and differentiated C2C12 cells. miR-135a levels were significantly reduced in differentiated C2C12 myotubes (Fig. 3A) together with an increase in the levels of its putative target, IRS2 (Fig. 3B, D). These suggest that as C2C12 myoblasts differentiate into myotubes, miR-135a levels show a pattern of down-regulation that might be responsible for the increased levels of its target, IRS2. Since, we had observed an inverse pattern of expression of miR-135a and IRS2, both in the tissues

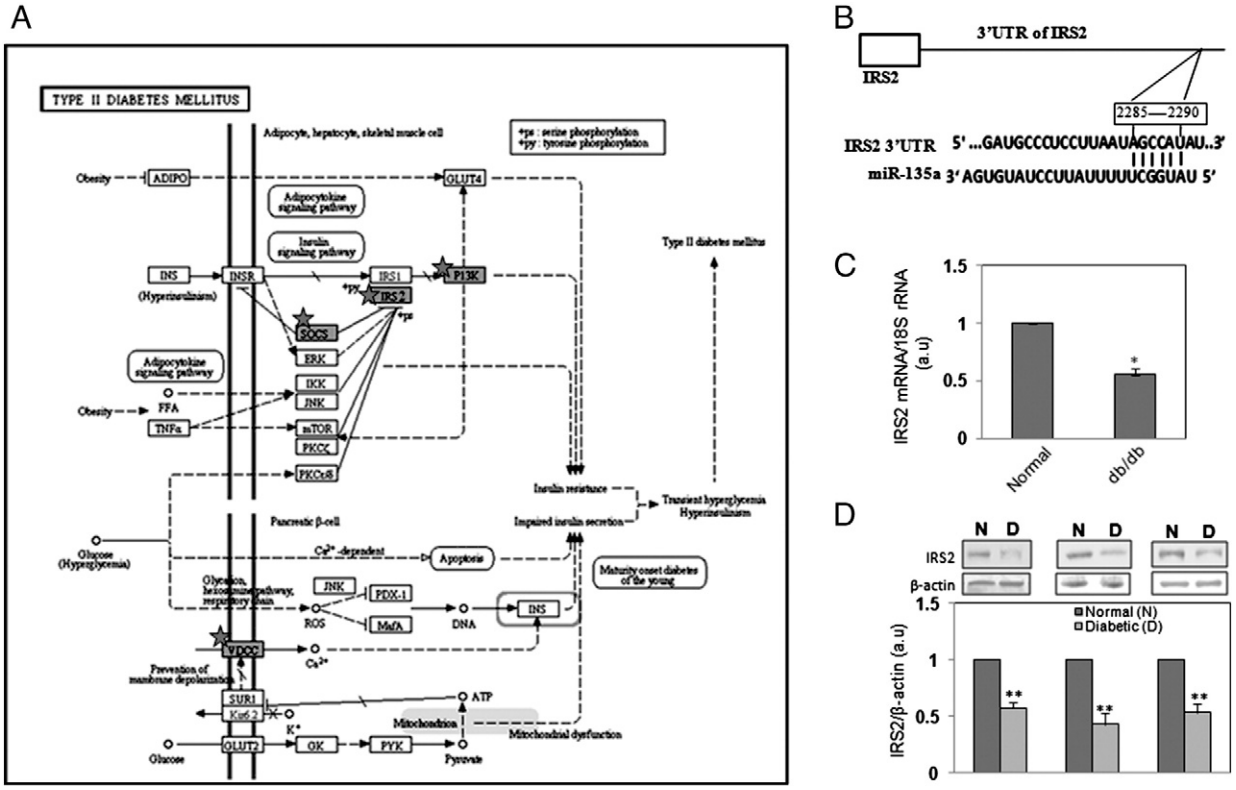

Fig. 2. The topmost pathway that the miR-135a targets enrich in and the levels of IRS2 in normal and diabetic skeletal muscle. (A) Schematic representation of the Type 2 diabetes pathway that was most significantly over-represented by the miR-135a targets' list. The grey shaded boxes with stars represent genes from the list of targets. (B) Schematic representation of the putative miR-135a binding site in the IRS2 3′UTR as in Targetscan. (C) Total RNA (2 μg) from normal and diabetic mice skeletal muscle were reverse transcribed and evaluated for IRS2 mRNA levels by quantitative RT-PCR using specific primers. (D) IRS2 protein levels were assessed in the normal (N) and diabetic (D) mice skeletal muscle. 50 μg protein of each sample were resolved by SDS-PAGE, transferred to nitrocellulose membranes and probed with anti-IRS2 antibody. A representative blot for each animal is given and the densitometric analysis is given below. Values are means ± SEM of triplicate experiments from each animal. $^{*}p < 0.05$ and $^{**}p < 0.01$ as compared to normal (non-diabetic) mice.

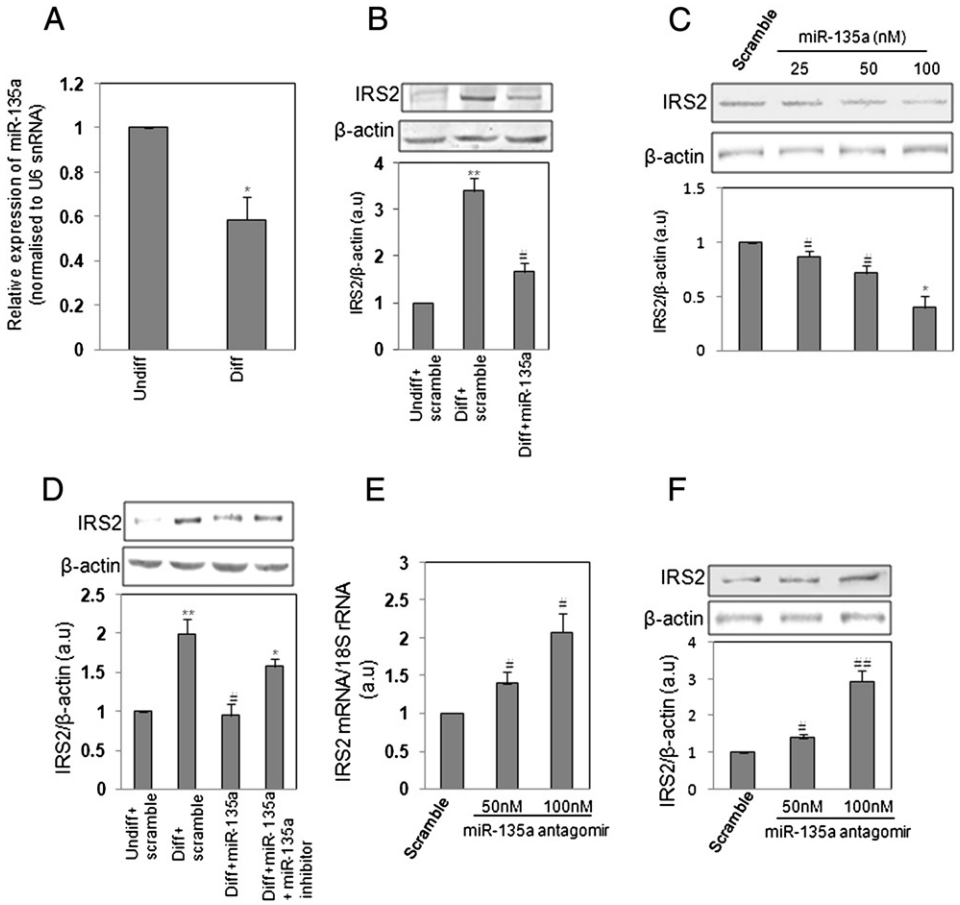

Fig. 3. miR-135a levels are decreased in differentiated C2C12 cells and they regulate cellular IRS2 levels. (A) C2C12 cells were differentiated into myotubes in the presence of 0.5% fetal bovine serum. The levels of miR-135a were assessed in these undifferentiated (undiff) and differentiated (diff) cells by quantitative Real-Time PCR using specific primers as given in the 'Materials and methods' section. (B) C2C12 cells were allowed to differentiate and were transfected with the scramble or miR-135a mimic (100 nM). On termination of incubation, cells were lysed and 50 μg protein from each incubation was resolved on SDS-PAGE and evaluated for the levels of IRS2 using anti-IRS2 antibody. β-Actin was taken as the loading control. (C) Differentiated C2C12 cells were transfected with miR-135a mimics at doses of 25–100 nM and incubated for 48 h. On termination of incubation, cells were lysed and the levels of IRS2 was assessed as in "B". β-Actin was taken as the loading control. (D) Cells were differentiated and incubated either in the absence or presence of miR-135a alone or miR-135a and its inhibitor (50 nM). On termination of incubation, cells were assessed for the status of IRS2 by Western Blot analysis. β-actin was taken as the loading control. C2C12 cells were transfected with miR-135a antagomir (50 and 100 nM) to knockdown endogenous miR-135a levels. After 48 h, the levels of IRS2 mRNA (E) and protein (F) were assayed by quantitative RT-PCR and Western Blot analysis where 18S rRNA and β-actin were taken as the loading controls, respectively. All experiments were done thrice and values are means ± SEM of three independent experiments. All blots shown are representatives of the indicated incubations and the densitometric analyses of the same are given below. $^{*}p < 0.05$ as compared to undifferentiated cells (A); $^{**}p < 0.01$ as compared to undifferentiated (undiff) cells and $^{\#}p < 0.01$ as compared to differentiated (diff) cells in the presence of scramble (B); $^{\#}p < 0.05$ and $^{*}p < 0.01$ as compared to differentiated cells incubated with the scramble (C); $^{**}p < 0.01$ as compared to undifferentiated cells, $^{\#}p < 0.05$ as compared to differentiated cells with scramble and $^{*}p < 0.05$ as compared to differentiated cells + miR-135a (D); $^{\#}p < 0.05$ and $^{\#\#}p < 0.01$ as compared to scramble (E and F).

(normal and diabetic) and C2C12 cells (undifferentiated and differentiated), we sought to delineate in detail whether IRS2 is functionally targeted by miR-135a. miR-135a mimics (100 nM) were transfected in differentiated C2C12 myotubes and as shown in Fig. 3B, miR-135a significantly reduced IRS2 protein expression. Also, incubation of C2C12 cells with miR-135a mimics from 25 to 100 nM depicted a dose-dependent decrease in IRS2 levels with the maximum decrease being evident at 100 nM (Fig. 3C) This decrease at 100 nM was blunted in the presence of the miR-135a inhibitor (Fig. 3D) suggesting the specificity of decreased IRS2 protein expression by miR-135a. To further confirm the specificity of this miR-135a–IRS2 interaction, we inhibited endogenous miR-135a levels using the miR-135a inhibitor at two doses of 50 and 100 nM. This was accompanied by a dose dependent increase in IRS2 at the transcript and protein levels (Fig. 3E, F). These results imply towards a specific interaction between miR-135a and IRS2 to regulate endogenous IRS2 levels.

Further, to test whether this decrease in IRS2 levels by miR-135a is due to miR-135a binding to the 3′UTR of IRS2, we cloned the 3′UTR of IRS2 into a psiCHECK-2 luciferase reporter vector. HEK cells were co-transfected with an empty vector or the 3′UTR IRS2 clone together with either the miR-135a mimic (5–50 nM) or a negative control (scramble). As compared to the scramble, miR-135a could significantly reduce the luciferase activity of the wild type IRS2 3′UTR reporter vector in a dose dependent manner (Fig. 4A). However, in the presence of the mutant IRS2 3′UTR reporter, miR-135a did not show any decrease in the luciferase activity at any of the doses used (Fig. 4A). Further, the miR-135a inhibitor significantly abrogated this decrease of the wild type IRS2 3′UTR luciferase activity (Fig. 4B) All these suggest that miR-135a decreases IRS2 levels by binding to its 3′UTR.

3.3. miR-135a over-expression attenuates insulin stimulated phosphorylation and activation of PI3K, Akt and glucose uptake

IRS2 is a critical mediator of the insulin signaling cascade. On being activated by the insulin receptor, it transmits the activation signal to downstream signaling mediators, PI3K and Akt that subsequently is translated into increased glucose uptake into skeletal muscles. Since we had observed an inhibition in IRS2 levels in the presence of miR-135a, we further studied the effect of this inhibition

on downstream effects of insulin action. Differentiated C2C12 cells were transfected with either the negative control (scramble) or miR-135a mimic, without or with its inhibitor, and then incubated in the absence or presence of insulin. In the presence of miR-135a, insulin stimulated phosphorylation of PI3Kp85α and Akt were significantly reduced (Fig. 5A, B). Also, these decreases were prevented in the presence of the miR-135a inhibitor. However, under all these conditions, the total levels of PI3kp85α and Akt were unaltered suggesting an effect of miR-135a only on insulin mediated phosphorylation of these proteins and not on their total levels.

Since the skeletal muscle is a major tissue responsible for glucose uptake, we subsequently studied the effects of these events on insulin stimulated glucose uptake in C2C12 cells. This was monitored by measuring the uptake of the glucose analogue, 2-(*N*-(7-nitrobenz-2-oxa-1,3-diazol-4-yl)amino)-2-deoxy-D-glucose (2-NBDG). While insulin significantly stimulated 2-NBDG uptake into C2C12 cells, this was abrogated by miR-135a (Fig. 5C). The specificity of this effect of miR-135a was assessed in the presence of the miR-135a inhibitor where the inhibitory effect of miR-135a on insulin stimulated glucose uptake was significantly rescued**.** All these suggest a specific effect of miR-135a on insulin signaling and glucose uptake by targeting IRS2.

Finally, in a step towards relating to human subjects, we assessed the levels of miR-135a in the normal and type 2 diabetic human skeletal muscles. As shown in Fig. 5D, miR-135a levels were significantly up-regulated in the skeletal muscle of human type 2 diabetic subjects. All these results suggest a critical role of the elevated levels of miR-135a in the diabetic skeletal muscle.

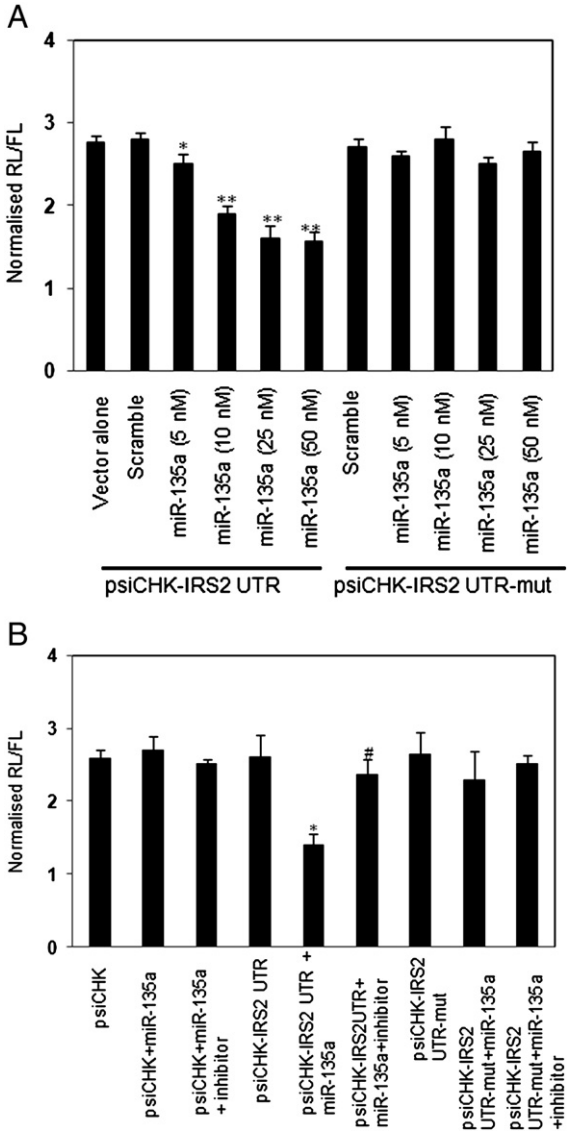

Fig. 4. miR-135a regulates IRS2 levels by binding to its 3′UTR. (A) HEK cells were seeded in 12-well plates and transfected with the vector alone or vector haboring the IRS2 3′UTR (wild type or mutated (mut) cloned in the psiCHECK2 (psiCHK) reporter vector) together with either the scramble or the miR-135a mimic (5–50 nM). After 48 h, cells were lysed and the Renilla (RL) and firefly luciferase activities was measured. (B) To check the specificity of the miR-135a effect, HEK cells were grown as in (A) and transfected with the scramble or miR-135a mimic (25 nM) alone or with its inhibitor (10 nM). Plasmids (150 ng) co-transfected with each of these sets were either the vector alone or that harboring the wild-type or mutant IRS2-3′UTR. Luciferase activities were determined as in "A". All experiments were done in triplicate. Renilla luciferase values that were normalized to those of firefly luciferase (FL) are expressed as means ± SEM. $^{*}p < 0.05$ and $^{**}p < 0.01$ as compared to cells with scramble (psiCHK-IRS2 UTR) and $^{\#}p < 0.05$ compared to cells incubated in the presence of miR-135a (psiCHK-IRS2 UTR + miR-135a).

3.4. Silencing of miR-135a in-vivo restores skeletal muscle IRS2 levels and improves circulatory blood glucose levels

To study the effect of miR-135a silencing *in-vivo*, we injected either the modified scramble or the miR-135a antagomir to normal and db/db mice at a dose of 80 mg/kg body weight for three consecutive days. As compared to the normal db/+ mice, diabetic db/db mice had significantly higher random glucose levels on each day of the experiment (Fig. 6A). However, as compared to the db/db mice injected with the scramble, injection of the miR-135a antagomir in db/db mice significantly decreased the blood glucose levels after the second dose of injection that further decreased after the third dose (Fig. 6A). Also, glucose tolerance tests showed an improved glucose tolerance in db/db mice injected with the miR-135a antagomir as compared to db/db mice injected with the scramble (Fig. 6B). These results suggest that miR-135a inhibition *in-vivo* alleviates hyperglycemia and improves glucose tolerance in the db/db mice. Further, in the gastrocnemius skeletal muscle of db/db mice injected with miR-135a antagomir, the levels of IRS2 was significantly restored (Fig. 6C). This was also accompanied by significant normalization of the levels p-Akt that lies downstream of IRS2 without any change in the total Akt levels. It has been suggested that antagomirs delivered intravenously through the tail vein are targeted to the liver and since hepatic insulin signaling also contributes to circulatory blood glucose levels, we also evaluated the status of IRS2, p-Akt and Akt in the livers of all the three groups of animals. As shown in Fig. 6C, the levels of IRS2 and p-Akt were significantly down-regulated in the livers of db/db mice. However, unlike the skeletal muscle, the hepatic IRS2 and p-Akt levels in mice injected with the miR-135a antagomir were not normalized and they remained comparable to those of scramble-treated db/db mice (Fig. 6C). Taken together, these data demonstrate that silencing of miR-135a *in-vivo* restores IRS2 levels in the gastrocnemius skeletal muscle of db/db mice and improves their hyperglycemic status. This improvement in the circulatory glucose levels is due to restoration of skeletal muscle IRS2 levels in the db/db mice injected with the miR-135a antagomir.

4. Discussion

Although there are several reports that describe the status and role of miRNAs in diabetic tissues, very few studies have focused on the diabetic skeletal muscle. The present study sought to evaluate the miRNA status in the gastrocnemius skeletal muscle of the diabetic db/db mice and to assess its physiological relevance.

The present data identified that, of the 41 miRNAs altered in the diabetic gastrocnemius skeletal muscle, 10 were up-regulated and 31 were down-regulated. Of these, miR-135a was one of the significantly up-regulated miRNAs and had targets predicted by TargetScan, PicTar and miRanda. These targets were significantly enriched in the "type 2 diabetes" pathway with the insulin signaling pathway

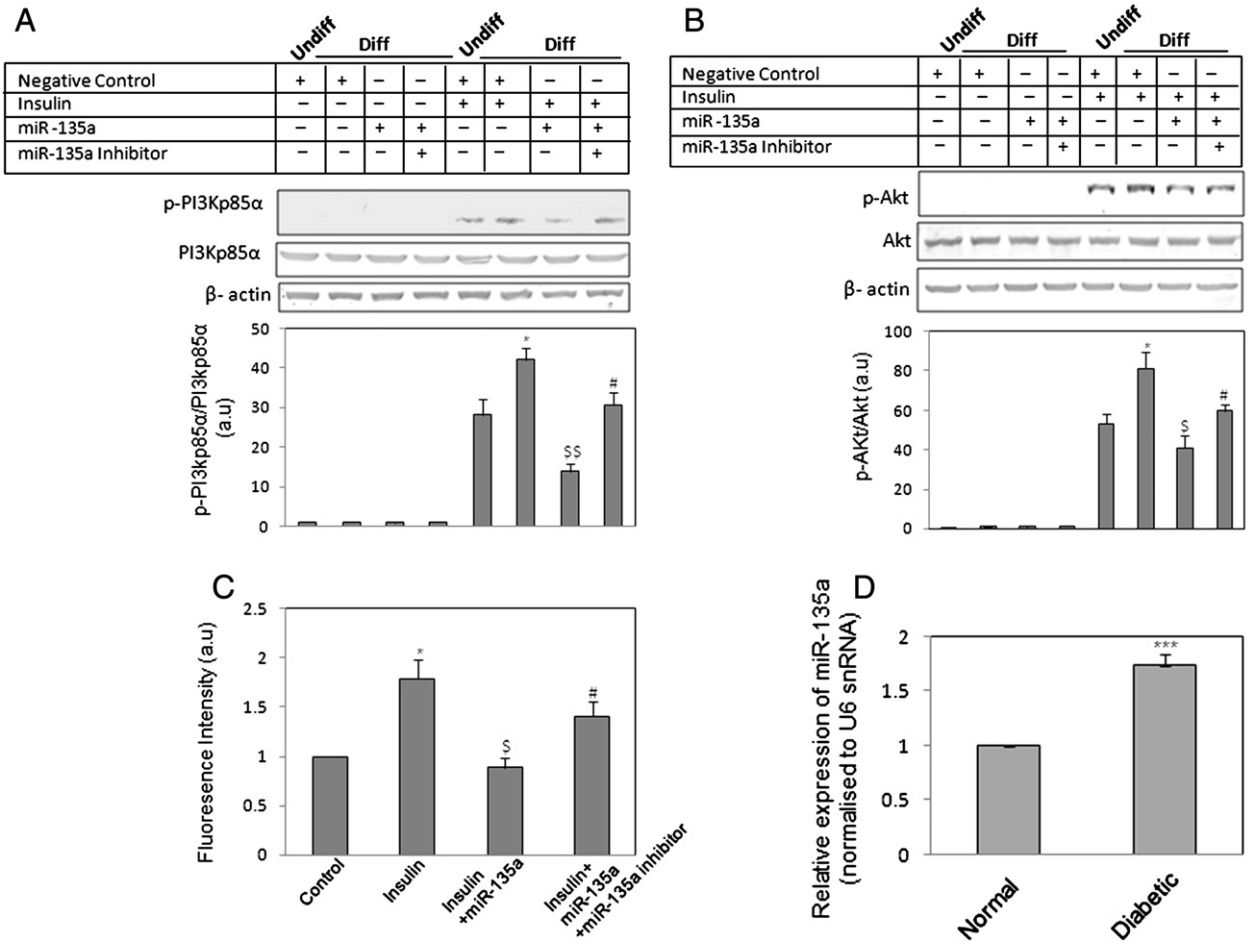

Fig. 5. Effect of miR-135a on insulin signaling in C2C12 cells and the status of miR-135a in the normal and diabetic human skeletal muscle. C2C12 cells were allowed to differentiate and transfected with either the scramble (negative control) or miR-135a mimic (100 nM) or the miR-135a mimic and its inhibitor (50 nM). After 48 h, cells were stimulated without or with insulin (100 nM) for 20 min and on termination of incubation, cells were lysed and lysates (50 μg) were subjected to Western Blot analysis using p-PI3Kp85α and PI3Kp85α (A) and p-Akt and Akt (B) antibodies. β-Actin was taken as the loading control. Each blot is a representative of three such independent blots and the densitometric data is given below. (C) To study the effect of miR-135a and its inhibitor on glucose uptake into C2C12 cells, differentiated C2C12 cells were transfected with the scramble or miR-135a with or without its inhibitor and stimulated with insulin for 10 min. Cells were then treated with insulin and 2-NBDG (500 μM) for 2 h at 37 °C, washed and the 2-NBDG uptake into the cell was evaluated by FACS analysis. (D) To determine the levels of miR-135a in the normal and diabetic human skeletal muscle, 2 μg of total RNA ($n = 3$ in each group) from each individual was reverse transcribed and the levels of miR-135a were determined by Real-Time PCR using specific primers as given in the "Materials and methods" section. All experiments were done thrice and representative figures are means ± SEM of three independent experiments. $^{*}p < 0.05$ as compared to undifferentiated (undiff) cells in the presence of insulin (A and B); $^{\$}p < 0.05$ and $^{\$\$}p < 0.01$ as compared to differentiated cells in the presence of insulin plus scramble; $^{\#}p < 0.05$ as compared to differentiated (diff) cells in the presence of insulin and miR-135a; $^{*}p < 0.01$ as compared to control (C); $^{***}p < 0.01$ as compared to normal (D).

harboring the maximum number of genes from the miRNA targets' list. mir-135a has been reported to be critical in skeletal muscle myogenesis primarily by regulating the levels of MEF2C [21]. MEF2C is a transcription factor that activates the expression of several muscle specific genes [28] and plays a significant role in myogenic differentiation [32] and in the maintenance of sarcomere integrity [33]. We, therefore, sought to study in detail, the role of elevated levels of miR-135a in the gastrocnemius skeletal muscle during diabetes. Although not in specific context of diabetes, miR-135a levels have been reported to be elevated in the inflammatory degenerative muscle [22] and to be significantly decreased in BMP induced differentiated osteoblasts [34]. Increased levels of miR-135a have been reported to increase the activity of caspase 3/7 and promote apoptosis [35].

As stated above, insulin signaling within the "type 2 diabetes" pathway was significantly enriched with genes from the miR-135a targets' list and here, IRS2 was a physiologically relevant target to be interested in. It harbors a binding site for miR-135a between 2285 and 2290 nucleotides on its 3′UTR (TargetScan). Here, we provide evidence that miR-135a regulates IRS2 levels by targeting its 3′UTR. IRS2 belongs to the IRS (insulin receptor substrate) family of proteins that interact with –SH2 domain containing proteins mainly PI3K during insulin action [36,37]. Specifically, IRS2 shares some structural and functional characteristics with IRS1. There are 22 potential tyrosine phosphorylation sites in human IRS2 and the presence of a unique region between 591 and 786 amino acids confers signaling specificity to this protein [38]. IRS2 null mice ($IRS2^{-/-}$), although normal at birth, show glucose intolerance and insulin resistance that gradually progresses to hyperglycemia [29,39]. These mice exhibit defects in muscle glycogen synthesis and impaired insulin action.

Our data show that while miR-135a levels are up-regulated in the db/db mice gastrocnemius skeletal muscle, IRS2 levels are correspondingly decreased. Using C2C12 myoblast cells, we prove that miR-135a decreases IRS2 levels by binding to its 3′UTR. The luciferase activity of the IRS2 3′UTR was significantly decreased in the presence of miR-135a and this decrease was markedly blunted in the presence of miR-135a inhibitor or in the presence of a mutation in the miR-135a binding site. To our knowledge, this is the first report to validate IRS2 as a key target of miR-135a.

Activation of IRS2 by binding of insulin to its receptor on the membrane initiates a signaling cascade that transmits through PI3K and Akt and subsequently facilitates glucose uptake into the cell [40]. We, therefore, sought to evaluate the physiological relevance

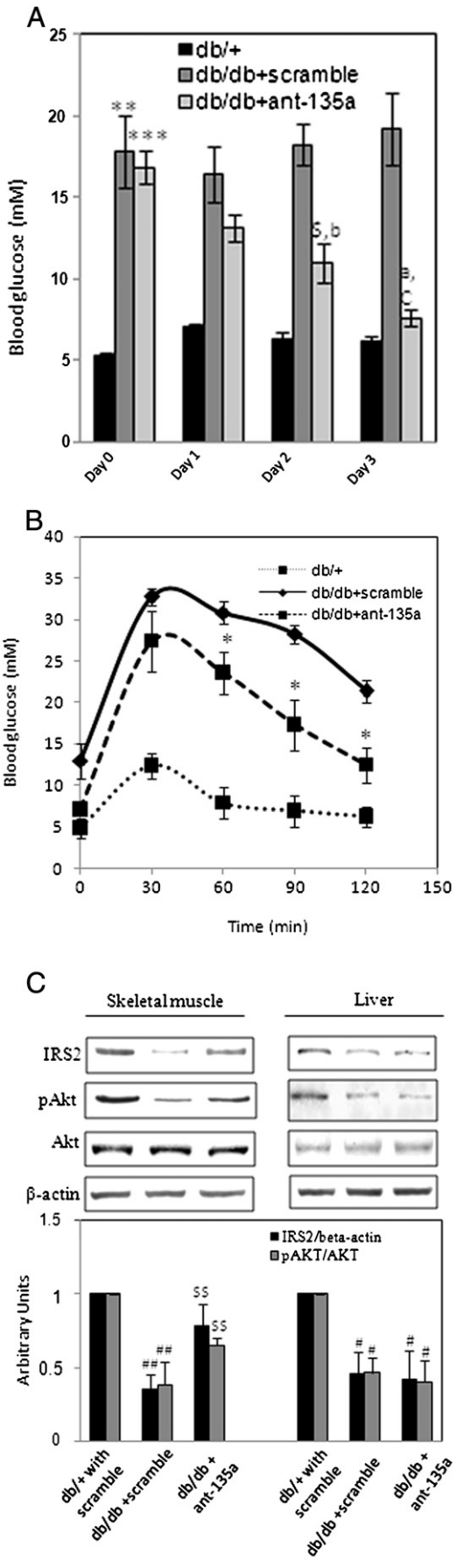

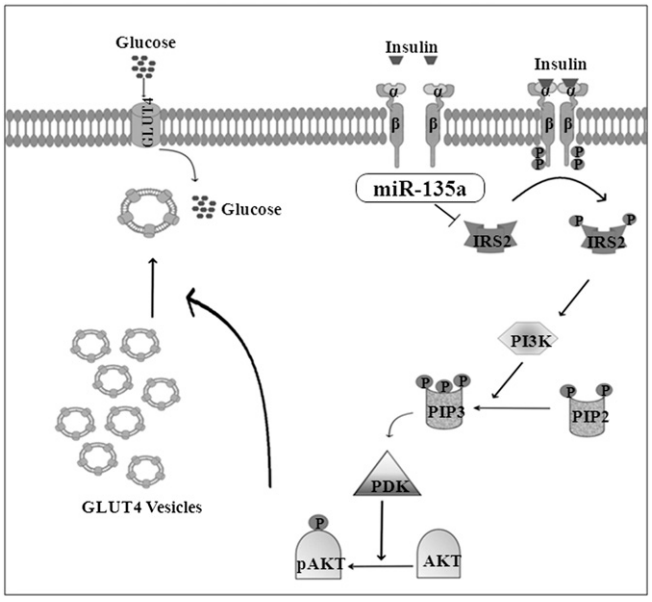

Fig. 7. Schematic representation of the role of miR-135a on the insulin signaling pathway. Insulin signaling begins by binding of insulin to its receptor on the membrane that initiates a cascade of signaling events within the cell. Insulin receptor (IR) phosphorylates and activates IRS2 followed by activation of PI3K that converts PIP2 to PIP3. This then activates a phospholipid dependent kinase, PDK, that regulates the phosphorylation and activation of Akt. p-Akt then facilitates the movement of Glut4 vesicles to the plasma membrane that promote the uptake of glucose into the cell. In the presence of miR-135a, IRS2 is inhibited that subsequently stalls the downstream insulin stimulated signaling events and finally glucose uptake into the cell is reduced. IR: Insulin receptor, IRS2: Insulin receptor substrate 2, PI3K: Phosphatidylinositol 3-kinase, PIP2: Phosphoinositide(4,5) bisphosphate, PIP3: Phosphoinositide(3,4,5)triphosphate, PDK: 3-Phosphoinositide-dependent Kinase, Akt: v-Akt murine thymoma viral oncogene, p-Akt-Phospho-Akt, Glut4: Glucose transporter type 4.

of the miR-135a–IRS2 pair in the skeletal muscle. Our results demonstrate that in the presence of miR-135a, insulin stimulated PI3K and Akt phosphorylation were significantly attenuated. Consequent to these, miR-135a also decreased insulin mediated glucose uptake into differentiated C2C12 cells. All these effects were abrogated in the presence of the miR-135a inhibitor indicating towards the specificity of these effects of miR-135a. *In vivo* injection of the miR-135a antagomir restored skeletal muscle IRS2 levels and also improved the hyperglycemic status of db/db mice. However, in the livers of db/db mice injected with the miR-135a antagomir, IRS2 and pAkt levels remained as comparable to the scramble-treated db/db mice liver. Also, in a recent report from our laboratory [18] regarding hepatic miRNA profiling in the same animals, miR-135a was not altered in the db/db mice liver suggesting that it might not be contributing to the decreased IRS2 levels in the db/db mice liver. These suggest that improved hyperglycemia that is observed in

Fig. 6. Silencing of miR-135a *in-vivo* alleviates hyperglycemia and improves the status IRS2 in the skeletal muscle. Diabetic db/db mice (n = 5 in each group) were injected with either the scramble or the miR-135a antagomir (ant-135a) at a dose of 80 mg/kg body weight for three consecutive days. Normal db/+ mice (n = 5) were also injected with the scramble in an identical manner. (A) Random blood glucose levels were measured on Day 0 (beginning of the experiment) and on each day of injection. (B) After the third injection, the animals were fasted overnight and were tested for oral glucose tolerance. (C) Skeletal muscle and liver tissues were dissected from each animal of all the groups and 50 μg protein was resolved through SDS-PAGE and IRS2, pAKT and AKT levels were detected by Western Blot analysis using specific antibodies. β-actin was used as the loading control. A representative blot is shown and below is the densitometric analysis of the data from 5 animals of each group. $^{**}p < 0.01$, $^{***}p < 0.001$ as compared to normal db/+ mice. $^{a}p < 0.01$, $^{b}p < 0.05$ as compared to Day 0 in db/db mice injected with ant-135a; $^{\$}p < 0.01$, $^{c}p < 0.001$ as compared to db/db mice injected with scramble for the same days. $^{*}p < 0.05$ as compared to respective time points in db/db animals injected with the scramble. $^{\#\#}$ $p < 0.01$ and $^{\#}p < 0.05$ as compared to normal db/+ mice with scramble and $^{\$\$}p < 0.05$ as compared to the respective proteins in db/db mice + scramble.

db/db mice injected with miR-135a antagomir is due to restoration of skeletal muscle IRS2 levels.

These results, therefore, provide novel insights into the role that miRNAs play in diabetes. The identification that miR-135a regulates insulin signaling by targeting IRS2 (Fig. 7) unravels one of the mechanisms that might be critical in the pathogenesis of insulin resistance and diabetes. This new role of miR-135a might open up new avenues to explore the therapeutic potential of miRNAs. IRS2 is a major intermediate during insulin signaling and its levels and activation are frequently inhibited in several diabetic species [30,41] and the fact that miR-135a targets IRS2 identify this miRNA as a novel metabolic regulator.

5. Conclusion

To conclude, the present study demonstrates that miR-135a is one of the significantly up-regulated miRNAs in the gastrocnemius skeletal muscle of diabetic db/db mice and by targeting IRS2, it interferes with insulin signaling and prevents insulin stimulated glucose uptake. This might contribute to the increased circulating glucose levels as observed in diabetic subjects. Our study, therefore, provides novel insights into the understanding of miRNA mediated alterations that might be critical to the onset and progression of diabetes.

Funding

We sincerely acknowledge the financial support from the Council of Scientific and Industrial Research (CSIR), New Delhi, India (BSC0123).

Acknowledgements

We are thankful to Saurabh Vig and Ankur Kulshreshtha for their help during the experiments. PA and RS acknowledge the Council of Scientific and Industrial Research (CSIR), New Delhi, India for their fellowships.

References

[1] D.P. Bartel, MicroRNAs: genomics, biogenesis, mechanism, and function, Cell 116 (2004) 281–297.
[2] R.C. Lee, R.L. Feinbaum, V. Ambros, The *C. elegans* heterochronic gene lin-4 encodes small RNAs with antisense complementarity to lin-14, Cell 75 (1993) 843–854.
[3] C. Zhao, G. Sun, S. Li, M.F. Lang, S. Yang, W. Li, Y. Shi, MicroRNA *let-7b* regulates neural stem cell proliferation and differentiation by targeting nuclear receptor TLX signaling, Proc. Natl. Acad. Sci. U. S. A. 107 (2010) 1876–1881.
[4] A.K. Pandey, P. Agarwal, K. Kaur, M. Datta, MicroRNAs in diabetes: tiny players in big disease, Cell. Physiol. Biochem. 23 (2009) 221–232.
[5] R.A. DeFronzo, D. Tripathy, Skeletal muscle insulin resistance is the primary defect in type 2 diabetes, Diabetes Care 32 (Suppl. 2) (2009) S157–S163.
[6] E. Phielix, M. Mensink, Type 2 diabetes mellitus and skeletal muscle metabolic function, Physiol. Behav. 94 (2008) 252–258.
[7] A.L. Carey, G.R. Steinberg, S.L. Macaulay, W.G. Thomas, A.G. Holmes, G. Ramm, O. Prelovsek, C. Hohnen-Behrens, M.J. Watt, D.E. James, B.E. Kemp, B.K. Pedersen, M.A. Febbraio, Interleukin-6 increases insulin-stimulated glucose disposal in humans and glucose uptake and fatty acid oxidation *in vitro* via AMP-activated protein kinase, Diabetes 55 (2006) 2688–2697.
[8] R.A. DeFronzo, D. Tripathy, Pathogenesis of type 2 diabetes mellitus, Diabetes Care 32 (Suppl. 2) (2009) S157–S163.
[9] L. Groop, C. Forsblom, M. Lehtovirta, T. Tuomi, S. Karanko, M. Nissen, B.O. Ehrnstrom, B. Forsen, B. Isomaa, B. Snickars, M.R. Taskinen, Metabolic consequences of a family history of NIDDM (the Botnia study): evidence for sex-specific parental effects, Diabetes 45 (1996) 1585–1593.
[10] G. Perseghin, T.B. Price, K.F. Petersen, M. Roden, G.W. Cline, K. Gerow, D.L. Rothman, G.I. Shulman, Increased glucose transport-phosphorylation and muscle glycogen synthesis after exercise training in insulin-resistant subjects, N. Engl. J. Med. 335 (1996) 1357–1362.
[11] C. Weyer, C. Bogardus, D.M. Mott, R.E. Pratley, The natural history of insulin secretory dysfunction and insulin resistance in the pathogenesis of type 2 diabetes mellitus, J. Clin. Invest. 104 (1999) 787–794.
[12] J.H. Warram, B.C. Martin, A.S. Krolewski, J.S. Soeldner, C.R. Kahn, Slow glucose removal rate and hyperinsulinemia precede the development of type II diabetes in the offspring of diabetic parents, Ann. Intern. Med. 113 (1990) 909–915.
[13] K.F. Petersen, S. Dufour, D.B. Savage, S. Bilz, G. Solomon, S. Yonemitsu, G.W. Cline, D. Befroy, L. Zemany, B.B. Kahn, X. Papademetris, D.L. Rothman, G.I. Shulman, The role of skeletal muscle insulin resistance in the pathogenesis of the metabolic syndrome, Proc. Natl. Acad. Sci. U. S. A. 104 (2007) 12587–12594.
[14] K. Bouzakri, H.A. Koistinen, J.R. Zierath, Molecular mechanisms of skeletal muscle insulin resistance in type 2 diabetes, Curr. Diabetes Rev. 1 (2005) 167–174.
[15] I.J. Gallagher, C. Scheele, P. Keller, A.R. Nielsen, J. Remenyi, C.P. Fischer, K. Roder, J. Babraj, C. Wahlestedt, G. Hutvagner, B.K. Pedersen, J.A. Timmons, Integration of microRNA changes *in vivo* identifies novel molecular features of muscle insulin resistance in type 2 diabetes, Genome Med. 2 (2010) 9.
[16] B. Huang, W. Qin, B. Zhao, Y. Shi, C. Yao, J. Li, H. Xiao, Y. Jin, MicroRNA expression profiling in diabetic GK rat model, Acta Biochim. Biophys. Sin. (Shanghai) 41 (2009) 472–477.
[17] D.S. Karolina, A. Armugam, S. Tavintharan, M.T.K. Wong, S.C. Lim, C.F. Sum, K. Jayaseelan, MicroRNA 144 impairs insulin signaling by inhibiting the expression of insulin receptor substrate 1 in type 2 diabetes mellitus, PLoS One 6 (2011) e22839.
[18] K. Kaur, A.K. Pandey, S. Srivastava, A.K. Srivastava, M. Datta, Comprehensive miRNome and in silico analyses identify the Wnt signaling pathway to be altered in the diabetic liver, Mol. Biosyst. 7 (2011) 3234–3244.
[19] K. McArthur, B. Feng, Y. Wu, S. Chen, S. Chakrabarti, MicroRNA-200b regulates vascular endothelial growth factor-mediated alterations in diabetic retinopathy, Diabetes 60 (2011) 1314–1323.
[20] D. Senador, K. Kanakamedala, M.C. Irigoyen, M. Morris, K.M. Elased, Cardiovascular and autonomic phenotype of db/db diabetic mice, Exp. Physiol. 94 (2009) 648–658.
[21] M. Cesana, D. Cacchiarelli, I. Legnini, T. Santini, O. Sthandier, M. Chinappi, A. Tramontano, I. Bozzoni, A long noncoding RNA controls muscle differentiation by functioning as a competing endogenous RNA, Cell 147 (2011) 358–369.
[22] S. Greco, M. De Simone, C. Colussi, G. Zaccagnini, P. Fasanaro, M. Pescatori, R. Cardani, R. Perbellini, E. Isaia, P. Sale, G. Meola, M.C. Capogrossi, C. Gaetano, F. Martelli, Common micro-RNA signature in skeletal muscle damage and regeneration induced by Duchenne muscular dystrophy and acute ischemia, FASEB J. 23 (2009) 3335–3346.
[23] M.W. Pfaffl, A new mathematical model for relative quantification in real-time RT-PCR, Nucleic Acids Res. 29 (2001) e45.
[24] Y. Chen, J. Zhang, H. Wang, J. Zhao, C. Xu, Y. Du, X. Luo, F. Zheng, R. Liu, H. Zhang, D. Ma, miRNA-135a promotes breast cancer cell migration and invasion by targeting HOXA10, BMC Cancer 12 (2012) 111.
[25] J. Wang, Y. Song, Y. Zhang, H. Xiao, Q. Sun, N. Hou, S. Guo, Y. Wang, K. Fan, D. Zhan, L. Zha, Y. Cao, Z. Li, X. Cheng, Y. Zhang, X. Yang, Cardiomyocyte over-expression of miR-27b induces cardiac hypertrophy and dysfunction in mice, Cell Res. 22 (2012) 516–527.
[26] N. Bossel Ben-Moshe, R. Avraham, M. Kedmi, A. Zeisel, A. Yitzhaky, Y. Yarden, E. Domany, Context-specific microRNA analysis: identification of functional microRNAs and their mRNA targets, Nucleic Acids Res. 40 (2012) 10614–10627.
[27] T.M. Witkos, E. Koscianska, W.J. Krzyzosiak, Practical aspects of microRNA target prediction, Curr. Mol. Med. 11 (2011) 93–109.
[28] Q. Lin, J. Schwarz, C. Bucana, E.N. Olson, Control of mouse cardiac morphogenesis and myogenesis by transcription factor MEF2C, Science 276 (1997) 1404–1407.
[29] D.J. Withers, J.S. Gutierrez, H. Towery, D.J. Burks, J.M. Ren, S. Previs, Y. Zhang, D. Bernal, S. Pons, G.I. Shulman, S. Bonner-Weir, M.F. White, Disruption of IRS-2 causes type 2 diabetes in mice, Nature 391 (1998) 900–904.
[30] M.J. Brady, IRS2 takes center stage in the development of type 2 diabetes, J. Clin. Invest. 114 (2004) 886–888.
[31] C.L. Sadowski, T.-S. Choi, M. Le, T.T. Wheeler, Lu-Hai Wang, H.B. Sadowski, Insulin induction of SOCS-2 and SOCS-3 mRNA expression in C2C12 skeletal muscle cells is mediated by Stat5, J. Biol. Chem. 276 (2001) 20703–20710.
[32] B. Lilly, B. Zhao, G. Ranganayakulu, B.M. Paterson, R.A. Schulz, E.N. Olson, Requirement of MADS domain transcription factor D-MEF2 for muscle formation in *Drosophila*, Science 267 (1995) 688–693.
[33] M.J. Potthoff, M.A. Arnold, J. McAnally, J.A. Richardson, R. Bassel-Duby, E.N. Olson, Regulation of skeletal muscle sarcomere integrity and postnatal muscle function by Mef2C, Mol. Cell. Biol. 27 (2007) 8143–8151.
[34] Z. Li, M.Q. Hassan, S. Volinia, A.J. van Wijnen, J.L. Stein, C.M. Croce, J.B. Lian, G.S. Stein, A microRNA signature for a BMP2-induced osteoblast lineage commitment program, Proc. Natl. Acad. Sci. U. S. A. 105 (2008) 13906–13911.
[35] A. Navarro, T. Diaz, A. Martinez, A. Gaya, A. Pons, B. Gel, C. Codony, G. Ferrer, C. Martinez, E. Montserrat, M. Monzo, Regulation of JAK2 by miR-135a: prognostic impact in classic Hodgkin lymphoma, Blood 114 (2009) 2945–2951.
[36] Y. Tsuji, Y. Kaburagi, Y. Terauchi, S. Satoh, N. Kubota, H. Tamemoto, F.B. Kraemer, H. Sekihara, S. Aizawa, Y. Akanuma, K. Tobe, S. Kimura, T. Kadowaki, Subcellular localization of insulin receptor substrate family proteins associated with phosphatidylinositol 3-kinase activity and alterations in lipolysis in primary mouse adipocytes from IRS-1 null mice, Diabetes 50 (2001) 1455–1463.
[37] G. Sesti, M. Federici, M.L. Hribal, D. Lauro, P. Sbraccia, R. Lauro, Defects of the insulin receptor substrate (IRS) system in human metabolic disorders, FASEB J. 15 (2001) 2099–2111.
[38] D. Sawka-Verhelle, S. Tartare-Deckert, M.F. White, O.E. Van, Insulin receptor substrate-2 binds to the insulin receptor through its phosphotyrosine-binding domain and through a newly identified domain comprising amino acids 591–786, J. Biol. Chem. 271 (1996) 5980–5983.
[39] S.F. Previs, D.J. Withers, J.-M. Ren, M.F. White, G.I. Shulman, Contrasting effects of IRS1 and IRS2 gene disruption on carbohydrate and lipid metabolism *in vivo*, J. Biol. Chem. 275 (2000) 38990–38994.
[40] L.F. del Aguila, K.P. Claffey, J.P. Kirwan, TNF-alpha impairs insulin signaling and insulin stimulation of glucose uptake in C2C12 muscle cells, Am. J. Physiol. 276 (1999) E849–E855.
[41] P. Vollenweider, B. Menard, P. Nicod, Insulin resistance, defective insulin receptor substrate 2-associated phosphatidylinositol-3′-kinase activation and impaired atypical protein kinase C (ζ/λ) activation in myotubes from obese patients with impaired glucose tolerance, Diabetes 51 (2002) 1052–1059.